The Extrinsic Anisotropy of Rock Salt when Subjected Simultaneously to Tensile and Compressive Stress Fields

E.K.S. Passaris

Department of Mining Engineering, University of Newcastle upon Tyne, Newcastle upon Tyne, England NE 1 7 RU

ABSTRACT

The design of underground, internally pressurized openings at shallow depths requires knowledge of the ultimate tensile strength and tensile constitutive relationship of the surrounding rock.

In order to investigate the behavior of rock salt in tension, under conditions similar to those predicted for internally pressurized openings, the hoop-stress loading test has been employed and found advantageous over other testing methods. However, the interpretation of the results of this test are involved, because of the simultaneous existence of tensile and compressive stress fields on the thick-walled cylindrical specimens. Neglecting this fact, and employing the classic analytical solution, which assumes that the constitutive behavior of the rock material is identical in compression and tension, leads to erroneous evaluation of the test results, due to an over-estimation of the tangential stresses. An analytical solution is developed, which takes into account the extrinsic anisotropy induced by the presence of compressive stresses along the radial direction and tensile stresses along the tangential direction in the hoop-stress loading test. The magnitude of error associated with the incorrect assumption of equal elastic constants in tension and compression is also investigated. The developed procedure of analytical evaluation of a hoop-stress loading test is illustrated in the case of rock salt, which is considered a typical example of a rock with different elastic constants in tension and compression.

The effect of the extrinsic anisotropy is considered as an important factor when employing hydrofracturing techniques or designing gas storage cavities in rocks where the elastic constants in tension and compression differ.

INTRODUCTION

A quantitative appreciation of the analysis of any rock mechanics problem is impossible, unless a knowledge of physical-mechanical properties of the associated rock materials can be established.

In problems linked with internally pressurized openings, i.e. hydro-power tunnels, underground gas storage cavities and hydro-fracturing techniques, the ultimate tensile strength and the constitutive description of the tensile stress-strain relationship is considered of paramount importance for the stability of the underground opening.

The tensile strength of any rock material is a complex subject. It is not apparently a unique property (although fundamentally it probably is) but is affected by the size of the specimen under test, its shape, the type of stress to be applied, the strain rate and the environmental conditions.

Rock salt, in particular, is known as being basically an aggregate of crystals embedded in marl, and most of its engineering properties, including tensile strength, depend on the structure of those crystals and the way in which they are bonded together. The behavior of the rock will also be affected by imperfections in the structure, such as voids (pore space), cracks, inclusions, crystal boundaries and weak particles.

In addition, structural factors are important, therefore, tending to overwhelm the mechanical variables and complicate the phenomenon of fracture on tension of rock salt. Consequently, in cases of internally pressurized openings, the study of the tensile strength should involve a testing procedure capable of simulating stress and geometrical boundary conditions similar to those predicted for the actual loading conditions. Accordingly, from all the different test

methods for evaluating tensile strength, the hoop-stress loading method is considered as the most appropriate.

The work which has been done on the determination of the tensile strength of rocks is quite impressive and numerous papers deal with this subject. In fact, a thorough comparison between the results given by direct pull, diametric compression of discs and annuli, and hoop-stress loading has been presented by Hardy and Jayaraman[1].

Tests carried out by other workers employing the hoop-stress loading technique have indicated that tensile failure of the thick walled cylindrical specimens occurs at stresses apparently considerably higher than the material's uniaxial tensile strength[2]. A similar phenomenon has been observed with tests conducted with Cheshire rock salt in the Department of Mining Engineering of the University of Newcastle upon Tyne and, in an attempt to offer an explanation of this apparent anomaly, an analytical solution based on extrinsic anisotropy caused by the simultaneous existing compressive and tensile stresses is presented.

EXPERIMENTAL METHOD AND RESULTS

Two large rock salt cylinders, with a ratio of internal to external radius of about 1:8, of inner diameter of 0.076 m, and a height of 0.254 m, have been internally pressurized to failure.

The loading of the specimens was achieved by pressurizing the inner surface of the cylinder by means of a hydraulic borehole radial expansion packer.

First specimen. The specimen was pressurized up to rupture in six incremental loading steps. After the peak of each step the pressure was dropped down to zero before starting the next step. Rupture occurred at the sixth step and at a pressure of 10.34 MPa. The history of loading can be seen in Figure 1 where the circumferential strain is plotted against induced pressure. The loading curve represents the average of the readings taken from a series of electrical resistance strain gauges mounted on the inner surface.

The readings from a set of gauges fixed on the outer surface showed no apparent deformation during the pressurization of the specimen; this supports the theoretical expectations on the stress distribution around a circular opening. A careful study of Figure 1 gives the following deductions:

1. The first loading shows a pressure-strain curve which is characterized by a concave upward slope. The radius of the curvature increases as the applied internal pressure increases. In other words, as the pressure increases, both Young's Modulus and Poisson's Ratio show an apparent increase that can be attributed to the closure of the open microcracks which are normal to the principal stresses.
2. After an internal pressure of 1 MPa the elastic constants remain unchanged in a region of linear reversible elasticity.

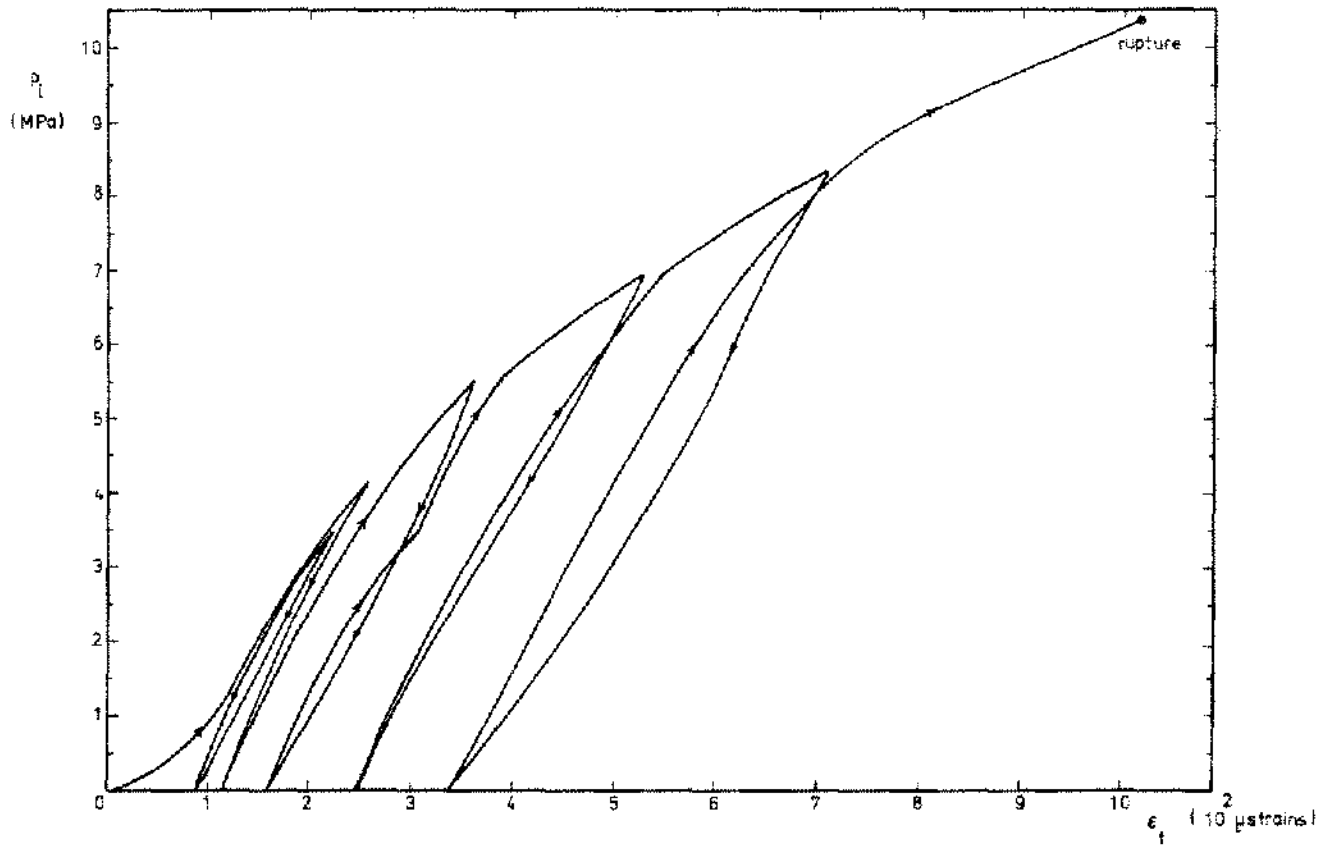

Figure 1. Internal pressure—tangential strain loading path for the first hollow cylindrical specimen.

3. The linear elastic region terminated when the internal pressure attained a critical value of 2.4 MPa, after which the increase in the applied internal pressure resulted in localized failures, i.e. microcracking. As can be seen from Figure 1, the pressure-strain graph beyond 2.4 MPa is markedly curved with the concavity directed towards the decreasing pressure. This curvature is caused by permanent changes in the microfabric of the rock. This can be seen clearly at the end of every unloading, where a permanent deformation set is recorded. It is also worth noting that the unloading paths show a linear deformation response since the presence of microcracks is no longer important, the crack propagation ceasing when load is removed.

Second specimen. During the testing of this specimen a geophone, stuck on the flat surface of the specimen near the hole, was used to monitor the microseismic activity during the test. This activity, which is often referred to as "acoustic emission" or "rock noise," is related to sudden releases of strain energy such as grain-boundary movement, or initiation and propagation of fractures through and between the grains.

The specimen was pressurized up to rupture in four stages of incremental loading. After the peak of each step the pressure was dropped down to zero before starting the next step. Rupture occurred at the fourth stage and at an internal pressure of 10.7 MPa. The pressure-strain path together with a qualitative representation of the microseismic activity is given in Figure 2. Up to the fourth loading stage, and including the 2.8 MPa pressure step, the loading curve represents the average of these readings taken from the three individual strain gauges mounted on the inner surface. Once the pressure of 2.8 MPa was exceeded, one of the gauges ceased to work, reducing the deformation readings to two. At the end of the experiment it was discovered that the rupture crack initiated from the location of the lost strain gauge.

A careful examination of Figure 2 leads to the following conclusions:

1. The three first loadings show a pressure-strain curve which follows a similar pattern to the one exhibited by the first specimen. Up to a pressure of 8.3 MPa the overall curve of the first specimen is identical to the curve of the second specimen.
2. An interesting part of the loading history is the fourth stage of pressurization. As soon as the critical value of 2.4 MPa was exceeded, a system of favorably orientated microcracks (which were initially formed when the pres-

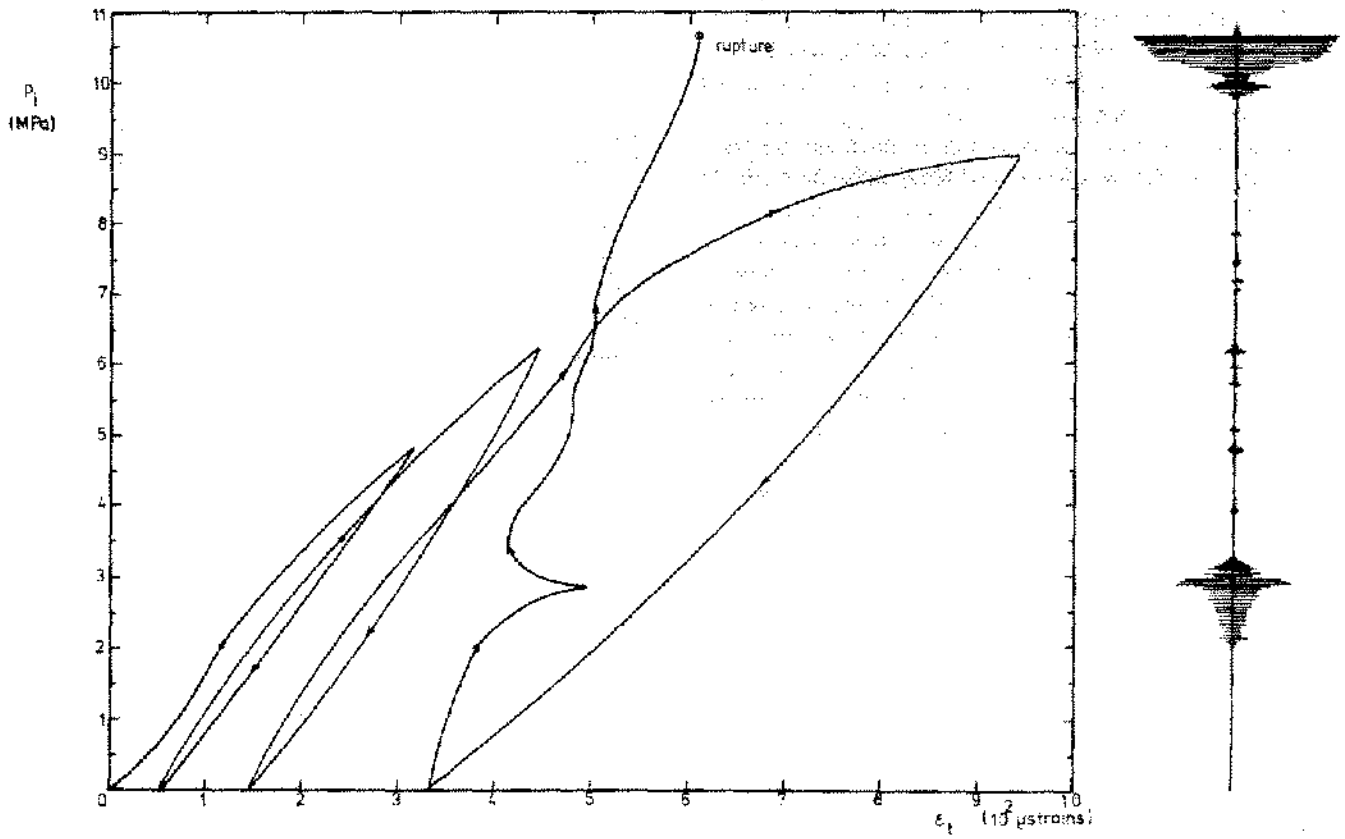

Figure 2. Internal pressure—tangential strain loading path, together with a qualitative representation of the microseismic activity of the second hollow cylindrical specimen.

sure increased beyond 2.4 MPa during the three previous loading stages) developed to a sizeable crack.

3. Because of the development of the crack up to a certain depth, the other inner surface gauges showed a sudden apparent strain recovery due to the surfaces stress relief by the crack.
4. It can be seen that the intensity of microseisms was directly connected with the initiation of the major crack and the final development of this crack into a structural failure of the specimen.

By comparing the two loading curves from Figure 1 and Figure 2 one can see that the strain-pressure path deviates from the linear elastic pattern as soon as a critical value of 2.4 MPa is exceeded. At this pressure (where microcracks initiated) the circumferential strain of the inner surface of the specimens was 150 micro-strains.

Taking into account the inner pressure at the moment of the initiation of failure was $p_i = 2.4$ MPa, then, on the basis of the dimensions of the specimens, the tensile stress at the inner surface of the specimen will be, according to Seely and Smith (3):

$$T_u = -1.031746\,(-p_i)$$

The above equation derived from the classical theory of Hookean elasticity yields a value for the ultimate tensile strength of rock salt of the order of 2.48 MPa, which is far from the value of 1.6 MPa that Dack (4) has determined experimentally for the same material.

If it is accepted that the detection of initial surface fracturing at 2.48 MPa was fortuitous, being dependent simply on the magnitude and location of the developed crack, it follows that undetected fracturing may have occurred at lower stresses equivalent to the uniaxial tensile strength. However, an increase in the internal pressure required to initiate fracturing could also occur if an extrinsic anisotropy with respect to radial and tangential direction exists because the elastic constants in tension are less than that in compression. Such a variation which is a property exhibited by most rock materials of very low tensile strength (5) would also lead to an apparently excessive deformation of the bore of the cylindrical specimens.

ANALYSIS

A linear elastic constitutive relation is developed for a material displaying a difference between compressive and tensile elastic constants, which in the case of a hoop-stress loading test may be treated as a transversely anisotropic material, since it will be in compression radially, and tension tangentially.

If the compressive Young's modulus and Poisson's Ratio are E_c, ν_c and the tensile values E_t, ν_t, then the isotropic Hookes Law in polar co-ordinates may be re-written for a plane stress analysis as (Appendix):

$$\sigma_t = E_c \frac{\epsilon_t + \epsilon_r}{(k-1)}\,,\ \sigma_r = E_c \frac{\epsilon_t + k\epsilon_r}{(k-1)}$$

where $k = \dfrac{E_t}{E_c}$

It may be shown that the stress components for the hoop-stress loading test can be expressed in terms of the dimensions of the specimen, the inner and outer pressure, and k, as follows (Appendix);

$$\sigma_r = (r^{x-1}(p_o r_i^{-x-1} - p_i r_o^{-x-1}) - (p_o r_i^{x-1} - p_i r_o^{x-1})r^{-x-1})/ /(r_i^{x-1} r_o^{-x-1} - r_i^{-x-1} r_o^{x-1})$$

$$\sigma_t = x(r^{x-1}(p_o r_i^{x-1} - p_i r_o^{-x-1}) + (p_o r_i^{x-1})r^{-x-1})/ /(r_i^{x-1} r_o^{-x-1} - r_i^{-x-1} r_o^{x-1}) \quad \ldots(1)$$

where $x = 1/\sqrt{k}$,

where $r_i = 38$ mm, $r_o = 305$ mm are the internal and external radii of the specimen, and p_i and $p_o = 0$ are the internal and external uniform pressures.

As was mentioned in the experimental results, at a critical inner pressure of 2.4 MPa an apparent failure—in the form of microcracks—was postulated for the inner surface of the specimen.

Using this pressure as the value of p_i, the tangential and radial stresses were calculated on the basis of equations (1) with the help of a computer program[6]. The resulting values, for different values of k, are plotted against the ratio r/r_i in Figure 3. Furthermore, the relationship between the circumferential stress on the inner surface of the cylinder and k is given in Figure 4.

The circumferential strain on the inner surface of the cylindrical specimen is obtained from equation (A1) of the Appendix as:

$$\epsilon_t = (k\sigma_t - \nu_c \sigma_r)/E_c\,,\ (\text{at } r = r_i) \qquad (2)$$

The compressive Young's Modulus of rock salt[7] is of the order of 36 GPa, and ϵ_t at $r = r_i$ was measured during the tests and found equal with 150 micro-strains at an internal pressure of 2.4 MPa. The radial stress σ_r at $r = r_i$ is equal with the applied internal pressure, and the value of σ_t at $r = r_i$ is taken from Figure 4, therefore the relation between k and Poisson's Ratio in compression can be determined using equation (2).

The resulting values are given in Figure 5, where the variation of k with ν_c can be seen, and employing a value of $\nu_c = 0.21$ that was determined for rock salt[7] then:

$$k = (E_c/E_t) = 3.6$$

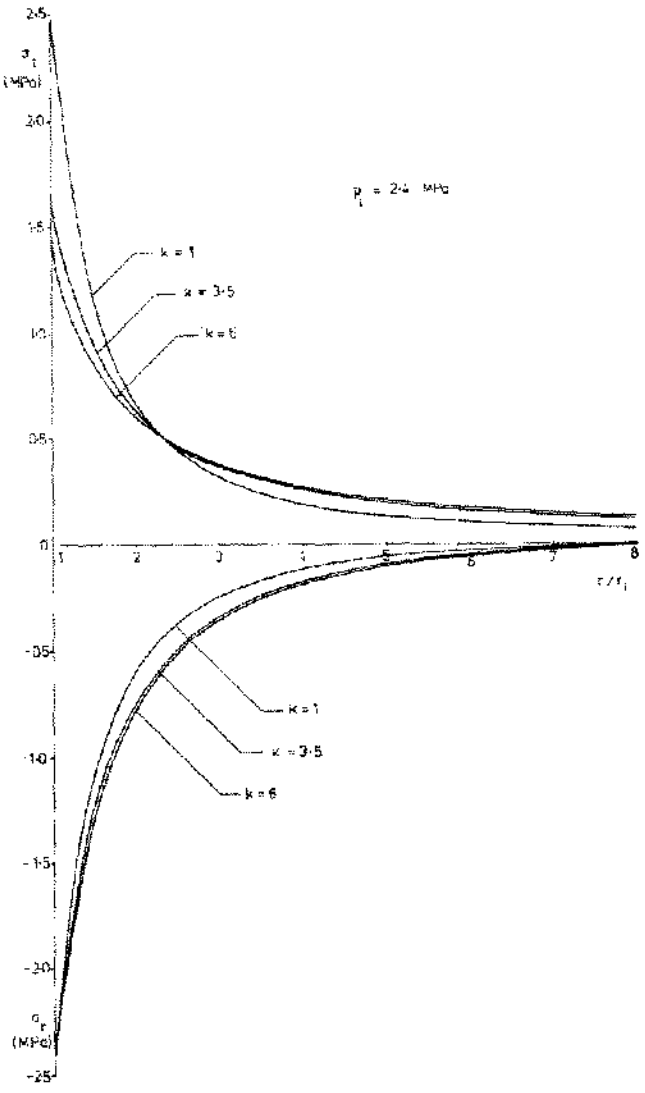

Figure 3. Stress distribution for thick welled cylinder for different values k (= E_o/E_i).

Furthermore one can see from Figure 4 that the tensile stress at the inner surface of the rock salt specimen at an inner pressure of 2.4 MPa for k = 3.6 is of the order of 1.6 MPa. It was mentioned before that at this pressure microcracks were formed on the inner surface, denoting the material's failure in tension, hence the tensile strength of rock salt corresponds to 1.6 MPa. This value agrees with the uniaxial tensile strength determined[4] for the same material.

If someone wants to explain the anomalous high value of the apparent tensile structural strength of the specimen (and not of the material), which allowed for internal pressures of the order of 10.7 MPa then the following approach[7] could be used.

If it is assumed that material failure occurs when any principle stress becomes equal to 1.6 MPa, then it may also be assumed that, within any volume where the stress value has been reached, the maximum possible stress in the appropriate direction will be equal to 1.6 MPa. This will lead to a "fractured zone" which is in many ways analogous to the "plastic zone" of the elastoplastic theory[2].

In the pressurized thick-walled cylindrical specimen this fracture zone will be bounded by a "fracture front" which and bounded internally by the inner surface. Externally the fractured zone will be bounded by a "fracture front" which will coincide with the limit of the critical stress value. As the internal pressure is increased this "fracture front" will propagate outwards, and when it coincides with the external surface of the specimen structural failure will occur.

Expressed in mathematical terms this theory states that in the fractured zone the equilibrium equation holds, and:

$$\sigma_t^* = T_u \quad \sigma_r^* = -p_i \quad \text{at } r = r_i$$

while in the intact zone where the boundary conditions are

$$\sigma_r = \sigma_r^*,\ \sigma_t = \sigma_t^* \text{ at } r = r_e \text{ and } \sigma_r = 0 \text{ at } r = r_o$$

where σ_r, σ_t are the radial and tangential stresses in the intact elastic region.

σ_r^*, σ_t^* are the radial and tangential stresses in the fractured zone

r_e is the fracture front radius

r_i, r_o are the internal and external radii of the cylindrical specimen, and

T_u is the ultimate uniaxial tensile strength of the material.

The equilibrium equation which is given in the Appendix when applied in the fractured zone has a solution

$$\sigma_r^* = (A/r) + T_u$$

where A is an arbitrary constant which can be defined from the boundary condition at $r = r_i$, hence

$$A = -r_i(T_u + p_i)$$

so that $\sigma_r^* = T_u\,(1-(r_i/r)) - (p_i r_i/r)$ (3)

If p_i is sufficiently small for the tangential stress at $r = r_i$ to be less than the uniaxial tensile strength, then the fracture front radius r_e will be equal to r_i and the stresses will be given by equations (1).

Structural failure will occur when the fracture front reaches the external surface so that $r_e = r_o$. But at $r = r_o$, $\sigma_r^* = 0$ hence equation (3) becomes:

$$p_i = T_u\,((r_o/r_i) - 1)$$

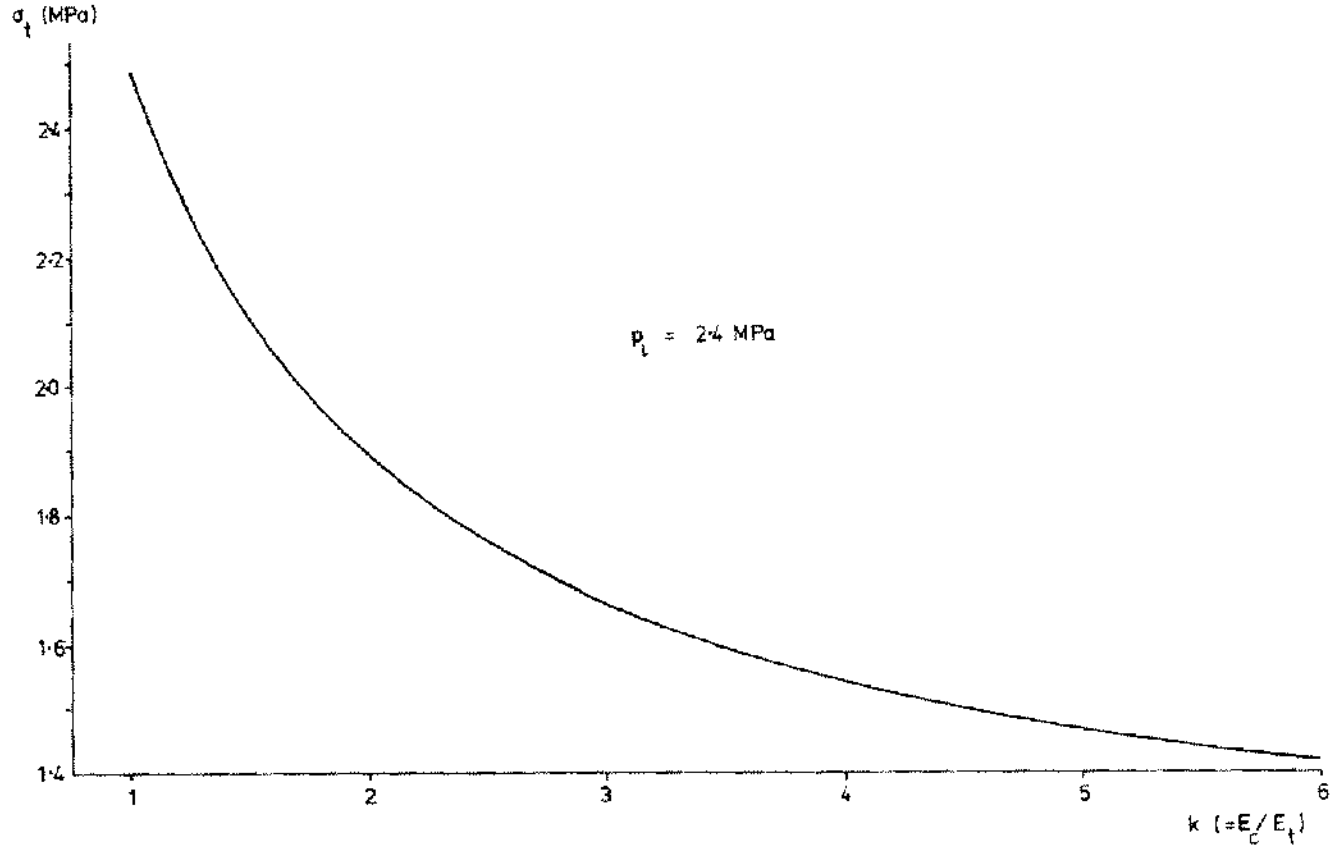

Figure 4. Variation of tangential stress with ratio of moduli in compression and tension.

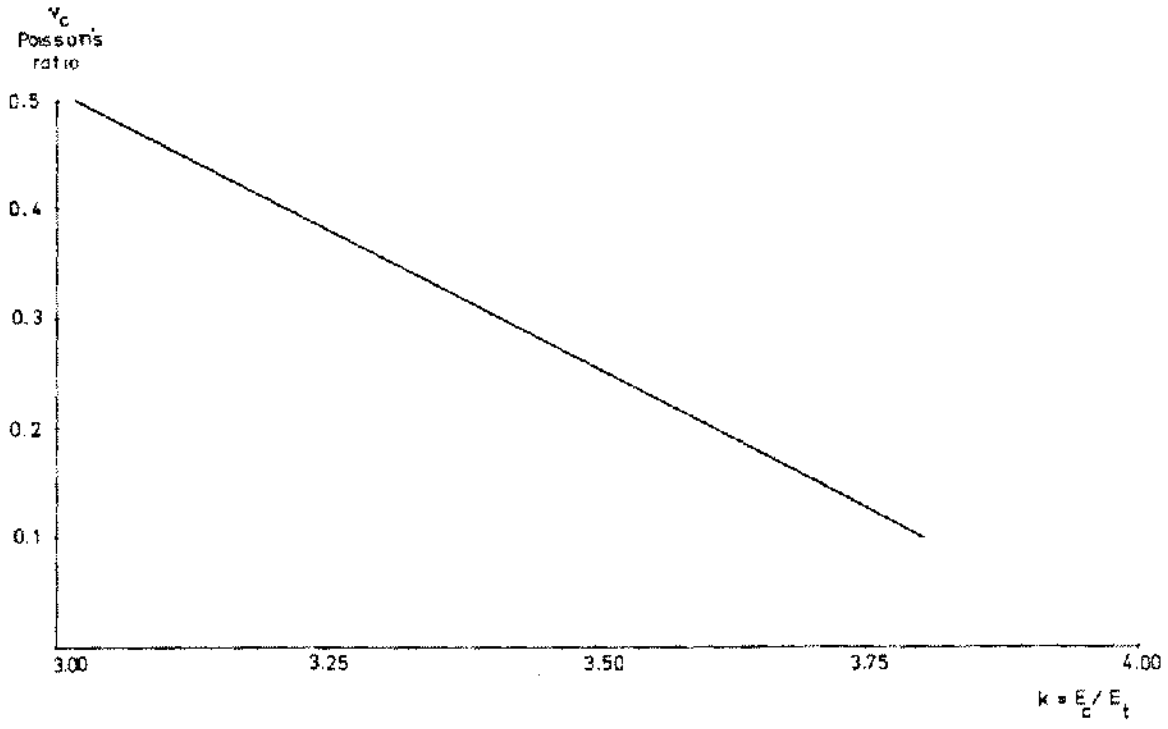

Figure 5. Variation of Poisson's ratio in compression with ratio of moduli in compression and tension.

which provides the inner pressure at which structural failure is expected. Substituting in the above relation a ratio of $(r_o/r_i) = 8$ and a value for $T_s = 1.6$ MPa, then:

$$p_i = 11.2 \text{ MPa}$$

which is within 5% of the observed values mentioned in the experimental results.

The structural fracture of the laboratory specimens therefore can be explained by the development of a fracture zone, the extent of which is determined by the internal pressure and limited by the inhomogeneity of the stress field.

CONCLUSIONS

Hoop-stress loading tests employing thick-walled cylindrical specimens offer a reliable method of determining the tensile strength of rocks surrounding internally pressurized underground openings. However, the interpretation of test results becomes involved because of the simultaneous existence of compressive stresses along radial direction and tensile stresses along the tangential direction. For rocks, like rock salt, possessing different constitutive relationships in tension and compression, thus developing an extrinsic anisotropy with respect to radial and tangential directions, the evaluation of the hoop-stress loading tests based on isotropic stress solutions leads to a considerable error in estimating their tensile strength.

To obtain the appropriate ultimate tensile strength, analytical solution obtained here by introducing the ratio of the elastic constants in tension and in compression, can be used.

The indicated analysis which was adopted to determine the constitutive relationships for rocks exhibiting extrinsic anisotropy is found to be satisfactory for the case of Cheshire rock salt.

The practical application of the developed theory is in the area of design of internally pressurized openings, i.e. hydro-power tunnels, underground gas storage cavities and hydrofracturing techniques.

APPENDIX

Assume a rectangular parallelepiped with its sides parallel to the co-ordinate axes acted upon by a normal tensile stress σ_1 uniformly distributed over two opposite sides. The magnitude of the normal strain ϵ_1 is given by

$$\epsilon_1 = \sigma_1/E_1$$

where E_1 is the modulus of elasticity in tension. Extension of the body in the direction 1 is accompanied by a lateral contraction in both 2 and 3 direction: thus

$$-\epsilon_2 = \nu_1(\sigma_1/E_1) \text{ and } -\epsilon_3 = \nu_1(\sigma_1/E_1)$$

where ν_1 is the Poisson's Ratio in tension.

If the rectangular parallelepiped is subject to a compressive stress σ_2 uniformly distributed over two opposite sides, the following relations are obtained

$$\epsilon_2 = (\sigma_2/E_2),\ -\epsilon_1 = \nu_2(\sigma_2/E_2),\ -\epsilon_3 = \nu_2(\sigma_2/E_2)$$

where ν_2 and E_2 are the Poisson's Ratio and elastic modulus in compression.

If the above parallelepiped is submitted simultaneously to the action of normal stresses σ_1, σ_2, σ_3 uniformly distributed over the sides, the resultant components of strain can be obtained if we superpose the strain components produced by each of the three stresses.

Hence:
$$\epsilon_1 = (\sigma_1/E_1) - \nu_2(\sigma_2/E_2) - \nu_3(\sigma_3/E_3)$$
$$\epsilon_2 = -\nu_1(\sigma_1/E_1) + (\sigma_2/E_2) - \nu_3(\sigma_3/E_3)$$
$$\epsilon_3 = -\nu_1(\sigma_1/E_1) - \nu_2(\sigma_2/E_2) + (\sigma_3/E_3)$$

It is noteworthy that σ_1 and σ_3 were both tensile therefore $E_1 = E_3$ and $\nu_1 = \nu_3$ consequently the above equations become:

$$\epsilon_1 = (\sigma_1/E_1) - \nu_2(\sigma_2/E_2) - \nu_1(\sigma_3/E_1)$$
$$\epsilon_2 = -\nu_1(\sigma_1/E_1) + (\sigma_2/E_2) - \nu_1(\sigma_3/E_1) \qquad \text{(A1)}$$
$$\epsilon_3 = -\nu_1(\sigma_1/E_1) - \nu_2(\sigma_2/E_2) + (\sigma_3/E_1)$$

and by using matrix representation the above equations are simplified into the following:

$$\begin{Bmatrix} \epsilon_1 \\ \epsilon_2 \\ \epsilon_3 \end{Bmatrix} = \begin{bmatrix} C_{11} & C_{12} & C_{13} \\ C_{21} & C_{22} & C_{23} \\ C_{31} & C_{32} & C_{33} \end{bmatrix} \begin{Bmatrix} \sigma_1 \\ \sigma_2 \\ \sigma_3 \end{Bmatrix}$$

However, it is known[8] that $C_{ij} = C_{ji}$ therefore $C_{12} = C_{21}$ and $C_{23} = C_{32}$. Consequently:

$$\nu_1/E_1 = \nu_2/E_2$$

or,
$$E_2/E_1 = \nu_2/\nu_1 = k \qquad \text{(A2)}$$

where k is the ratio of elastic moduli in compression and tension.

Taking into account the above equation the stress-strain equations becomes:

$$\epsilon_1 = (\sigma_1/E_1) - \nu_2(\sigma_2/E_2 - \nu_1(\sigma_3/E_1)$$
$$\epsilon_2 = -\nu_2(\sigma_1/E_2) + (\sigma_2/E_2) - \nu_2(\sigma_3/E_2) \qquad \text{(A3)}$$
$$\epsilon_3 = -\nu_1(\sigma_1/E_1) - \nu_2(\sigma_2/E_2) + (\sigma_3/E_1)$$

Applying the concept of plane stress over the (1, 2) plane, σ_3 becomes zero, hence:

$$\epsilon_1 = \sigma_1 \frac{1}{E_1} - \sigma_2 \frac{\nu_2}{E_2}$$

$$\epsilon_2 = -\sigma_1 \frac{\nu_2}{E_2} + \sigma_2 \frac{1}{E_2}$$

and using equation A2 while setting $E = E_1$ and $\nu = \nu_1$ we get:

$$\epsilon_1 = \sigma_1 \frac{1}{E} - \sigma_2 \frac{\nu}{E}$$

$$\epsilon_2 = \sigma_1 \frac{\nu}{E} + \sigma_2 \frac{1}{kE}$$

Rewriting the above equations in order to express stresses in terms of strain we have:

$$\sigma_1 = \frac{E}{1-k\nu^2}(\epsilon_1 - k\nu\epsilon_2)$$

$$\sigma_2 = \frac{kE}{1-k\nu^2}(\epsilon_2 + \nu\epsilon_1) \qquad (A4)$$

Let us now consider a cylinder, whose inner and outer radii are r_i and r_0, and whose inner and outer surfaces are acted upon by uniform pressures $-p_i$ and $-p_0$ respectively

Taking into account the symmetrical nature of the internal and external hydrostatic loading it is obvious that the shear stresses are zero, hence the equilibrium equation is reduced into:

$$\sigma_t - \sigma_r - r(d\sigma_r/dr) = 0 \qquad (A5)$$

In addition to fulfilling the equilibrium requirements, the strains must be compatible and satisfy the constitutive relations. If u is the displacement of the material at radius r, then $(u - (du/dr)dr)$ is the displacement of the material of radius $(r + dr)$. Thus the strain-displacement equations are

$$\epsilon_r = (u + (du/dr)\,dr - u)\,dr = du/dr$$

$$\epsilon_t = ((r+u)\,dt - rdt)\,rdt = u/r \qquad (A6)$$

where ϵ_r and ϵ_t are strains in the radial and tangential directions.

Using equations (A4) and substituting subscript 1 for t and subscript 2 for r we get:

$$\sigma_t = \frac{E}{1-k\nu^2}(\epsilon_t - k\nu\epsilon_r)$$

$$\sigma_r = \frac{kE}{1-k\nu^2}(\epsilon_r + \nu\epsilon_t) \qquad (A7)$$

If we substitute equations (A6) in equations (A7) we get

$$\sigma_t = \frac{E}{1-k\nu^2}\left(\frac{u}{r} + k\frac{du}{dr}\right) \qquad (A8)$$

$$\sigma_r = \frac{kE}{1-k\nu^2}\left(\frac{du}{dr} + \nu\frac{u}{r}\right) \qquad (A9)$$

Using equations (A8), and (A9) the equilibrium equation (A5) may be written:

$$k\frac{d^2u}{dr^2} + k\frac{1}{r}\frac{du}{dr} - \frac{u}{r^2} = 0 \qquad (A10)$$

and since $k \neq 0$ we can divide by k and we get:

$$\frac{d^2u}{dr^2} + \frac{1}{r}\frac{du}{dr} - \frac{1}{k}\frac{u}{r^2} = 0$$

The above equation is a homogeneous linear differential equation, which if multiplied by r^2 becomes a second order Euler equation.

$$r^2u'' + ru' - u\frac{1}{k} = 0$$

By setting $r = \exp(t)$, then $u'' = (\ddot{u} - \dot{u})\exp(-2t)$ and $u' = \dot{u}\exp(-t)$, where the dot denotes differentiation over t, and the above equation yields

$$\ddot{u} - \frac{1}{k}u = 0 \qquad (A11)$$

The characteristic equation of (A11) is

$$Z^2 - \frac{1}{k} = 0$$

hence $$Z = \pm 1/\sqrt{k} \qquad (A12)$$

And by setting

$k = \frac{1}{x^2}$ the complementary integral of (A10) is given as

$$u = C_1\exp(xt) + C_2\exp(-xt)$$

but since $r = \exp(t)$, then $t = \ln(r)$, consequently

$$u = C_1r^x + C_2r^{-x} \qquad (A13)$$

Since the right hand side of equation (A11) is zero the particular integral is zero, and so equation (A13) is the general integral of equation (A10), and the stress components are now found by using the solution (A13) in equations (A8) and (A9).

$$\sigma_t = xE\left(C_1\frac{r^{x-1}}{x-\nu} + C_2\frac{r^{-x-1}}{x+\nu}\right) \qquad (A14)$$

$$\sigma_r = E\left(C_1\frac{r^{x-1}}{x-\nu} - C_2\frac{r^{-x-1}}{x+\nu}\right) \qquad (A15)$$

The constants C_1, C_2 are determined by the boundary conditions:

$$\sigma_r = -p_i \text{ at } r = r_i$$

$$\sigma_r = -p_0 \text{ at } r = r_0.$$

Therefore from equation (A15)

$$C_1 = \frac{(\varkappa+\nu)(p_i r_o^{\varkappa-1} - p_o r_i^{\varkappa-1})}{\varkappa E(r_i^{-\varkappa-1} r_o^{\varkappa-1} - r_i^{\varkappa-1} r_o^{-\varkappa-1})}$$

$$C_2 = \frac{(\varkappa+\nu)(p_i r_o^{\varkappa-1} - p_o r_i^{\varkappa-1})}{\varkappa E(r_i^{-\varkappa-1} r_o^{\varkappa-1} - r_i^{\varkappa-1} r_o^{-\varkappa-1})}$$

Substituting the above relations in equations (A14) and (A15) and using equation (A12) we find the expressions

$$\sigma_r = (r^{\varkappa-1}(p_o r_i^{\varkappa-1} - p_i r_o^{\varkappa-1}) - (p_o r_i^{\varkappa-1} - p_i r_o^{\varkappa-1}) r^{-\varkappa-1})/$$
$$/(r_i^{\varkappa-1} r_o^{-\varkappa-1} - r_i^{-\varkappa-1} r_o^{\varkappa-1})$$

$$\sigma_t = \varkappa(r^{\varkappa-1}(p_o r_i^{-\varkappa-1} - p_i r_o^{-\varkappa-1}) + (p_o r_i^{\varkappa-1} - p_i r_o^{\varkappa-1}) r^{-\varkappa-1})/$$
$$/(r_i^{\varkappa-1} r_o^{-\varkappa-1} - r_i^{-\varkappa-1} r_o^{\varkappa-1}).$$

REFERENCES

1. Hardy, H.R. Jr. and Jayaraman, N.I. 1970. An investigation of methods for the Determination of the Tensile Strength of rock. 2nd Cong. Rock Mech. Proc., Beograd.
2. Jaeger, J.C. and Cook, N.G. 1971. Fundamentals of Rock Mechanics. Chapman & Hall Ltd., London.
3. Seely, F.B. and Smith, J.O. 1952. Advanced Mechanics of Materials Wiley, New York.
4. Dack, E. 1973. An "In-situ" Investigation of the Physical Properties of Rocksalt with Special Reference to Underground Gas Storage. Ph.D. Thesis, Dept. of Min. Eng., Newcastle Univ., U.K.
5. Boffinger, H.E. 1970. The Measurement of the Tensile Properties of Soil-Cement, Rep. L.R. 365, Ministry of Transport, Road Research Lab., Crowthorne, Berks.
6. Passaris, E.K.S. 1975. The Storage of Gas in Deep Solution Mined Cavities in Halite. Ph.D. Thesis, Dept. of Mining Eng., Univ. of Newcastle upon Tyne, U.K.
7. Potts, E.L.J. et al. 1975. Gas Storage in Brine Well Cavities, Final Report to I.C.I. Dept. of Mining Eng., Univ. of Newcastle upon Tyne, U.K.
8. Green, A.E. and Zerna, W. 1968. Theoretical Elasticity. Oxford University Press.